

**Atf İçin:** Gungör E, Sevinç R, Kara Subaşat H, 2021. Piridin-4-Boronik Asit Katyonu ve Pt(CN)<sub>4</sub> Anyon Tuzunun Yeni Bileşiği: Sentez, Yapısal Özellikler, Hirshfeld Yüzey Analizi ve Yoğunluk Fonksiyonel Teori Hesaplamaları. İğdır Üniversitesi Fen Bilimleri Enstitüsü Dergisi, 11(3): 1990-2000.

**To Cite:** Gungor E, Sevincek R, Kara Subasat H, 2021. New Compound of Pyridine-4-Boronic Acid Cation and Pt(CN)<sub>4</sub> Anion Salt: Synthesis, Structural Properties, Hirshfeld Surface Analysis and Density Functional Theory Calculations. Journal of the Institute of Science and Technology, 11(3): 1990-2000.

## New Compound of Pyridine-4-Boronic Acid Cation and Pt(CN)<sub>4</sub> Anion Salt: Synthesis, Structural Properties, Hirshfeld Surface Analysis and Density Functional Theory Calculations

Elif GUNGOR<sup>1\*</sup>, Resul SEVINCEK<sup>2</sup>, Hulya KARA SUBASAT<sup>3</sup>

**ABSTRACT:** In this work, the novel compound [HNC<sub>5</sub>H<sub>4</sub>B(OH)<sub>2</sub>-4][Pt(CN)<sub>4</sub>] (**1**) has been synthesized and structurally characterized. The compound (**1**) crystallizes in monoclinic, space group *P2<sub>1</sub>/c*, *a*=5.6159(11) Å, *b*=14.656(3) Å, *c*=11.619(2) Å,  $\alpha=90^\circ$ ,  $\beta=110.35(3)$ ,  $\gamma=90^\circ$ , *V*= 896.6(3) Å<sup>3</sup>, *Z*=2. The optimum molecular geometry parameters have been investigated with the DFT/B3LYP method. All geometric parameters are found in good agreement with crystallographic and computational results. Contributions of fragments molecular orbitals (HOFO-LUFO) to frontier molecular orbitals (HOMO-LUMO) are calculated charge transferred from Pt moiety to other fragments.

**Keywords:** Boroxine compound, DFT calculations, Hirshfeld surface analysis

<sup>1</sup>Elif GUNGOR ([Orcid ID: 0000-0002-7158-9604](https://orcid.org/0000-0002-7158-9604)), Balıkesir University, Faculty of Science and Art, Department of Physics, Balıkesir, Turkey

<sup>2</sup>Resul SEVINCEK ([Orcid ID: 0000-0001-6859-0287](https://orcid.org/0000-0001-6859-0287)), Dokuz Eylul University, Faculty of Science, Department of Physics, Izmir, Turkey

<sup>3</sup>Hulya KARA SUBASAT ([Orcid ID: 0000-0002-2032-8930](https://orcid.org/0000-0002-2032-8930)), Muğla Sıtkı Kocman University, Graduate School of Natural and Applied Sciences, Department of Energy, Muğla, Turkey

\* Corresponding Author: Elif GUNGOR, e-mail: egungor@balikesir.edu.tr

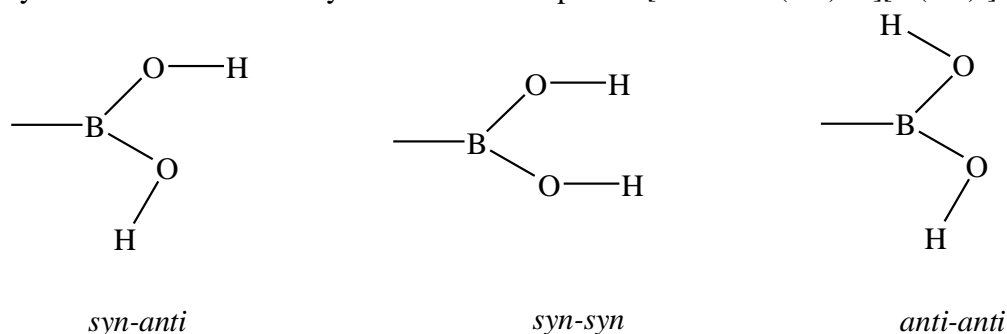
## INTRODUCTION

The boronic acids are important substances for organic transformations and are known to be primary precursors in bioorganic and medicinal chemistry (Miyaura and Suzuki, 1995; Hall, 2011). They have popular cross-coupling properties in natural product synthesis and medicinal chemistry (Suzuki et al., 1998; Roughley and Jordan, 2011; Li et al., 2019; Diccianni and Diao, 2019; Deng et al., 2020; Mohammadi and Ghorbani-Choghamarani, 2020). Because these properties have been used in the structure of several pharmaceutical drugs. Several boronic acids have been evaluated as sources of boron for their potential use in a form of cancer therapy (Yang et al., 2003; Deagostino et al., 2016; Zhu et al., 2020; Kumar et al., 2020). Also, boronic acids are generally used in the field of agrochemicals (Torborg and Beller, 2009), organic chemistry (Yang et al., 2002; Ejsmont et al., 2003), inhibitors of proteases (Khangulov et al., 1995; Carvajal et al., 1996). Therefore, this research addresses the synthesis and crystallization of magnetic materials with the use of boronic acid ligands.

Although the use of boronic acid has seen an increase in different industries, it finds limited application in the field of super chemistry. There are very few studies in supermolecular systems that contain hydrogen bonds in derivatives of carboxylic and boronic acid (Kara et al., 2006; Campos-Gaxiola et al., 2010). Therefore, to form different variants of the supramolecular group by pursuing crystal engineering principles, this research on pyridine boronic acids with metal complex anions has been proposed where synthesis and molecular recognition of supramolecules and hydrogen bond interactions between component tectons have examined.

The boronic acid has been three types of conformation in the literature as *syn-anti*, *syn-syn*, and *anti-anti* (Scheme 1) (Varughese et al., 2011; Yahsi et al., 2015). These conformations enable the formation of a variety of hydrogen-bonded networks according to different arrangements of two hydroxyl groups. The *syn-anti*-conformation from these arrangements is observed in most structures while *syn-syn* and *anti-anti*-conformations are rare (SeethaLekshmi and Pedireddi, 2007; Yahsi et al., 2015).

Recently, our research group has been actively working on the structural and photoluminescence properties of molecules containing various aromatic carboxylate and pyridine derivatives for the past few years (Erkarlan et al., 2016; Coban et al., 2016; Kocak et al., 2017; Erkarlan et al., 2018). We have previously reported a range of charge-assisted hydrogen-bonded aggregations based on [MCl<sub>4</sub>]<sup>2-</sup> (M = Ni, Cu, Pt, and Pd) anionic salts with 3- and 4-pyridine boronic acid cations (Yahsi et al., 2015). These studies show that cations allow the synthesis of hydrogen-bonded networks due to their hydrogen bond donating abilities. Therefore, in this study, we have report synthesis, crystal structure and intermolecular interactions by Hirshfeld surface analysis of a new compound [HNC<sub>5</sub>H<sub>4</sub>B(OH)<sub>2</sub>-4][Pt(CN)<sub>4</sub>] (**1**).



**Scheme 1**

## MATERIALS AND METHODS

### Materials and measurements

[HNC<sub>5</sub>H<sub>4</sub>B(OH)<sub>2-4</sub>][PtCN<sub>4</sub>] was prepared according to the published procedure (Kara et al., 2006). A three-circle CCD diffractometer containing Mo-K $\alpha$  radiation was used to collect single-crystal X-ray diffraction data. Then, the measured intensity data were made with the SAINT program (Bruker-AXS, 2008) absorption, Lorentz, and polarization corrections. The structure of compound solved with SHELXTL (Sheldrick, 2008) in OLEX2 program (Dolomanov et al., 2009). Hydrogen atoms were included in idealized positions.

### Syntheses of [HNC<sub>5</sub>H<sub>4</sub>B(OH)<sub>2-4</sub>][PtCN<sub>4</sub>] (1)

[HNC<sub>5</sub>H<sub>4</sub>B(OH)<sub>2-4</sub>][PtCN<sub>4</sub>] (1) was synthesized by mixing of pyridine-4-boronic acid hydrochloride (34.7 mg, 0.21 mmol) in 5 ml of water and K<sub>2</sub>PtCN<sub>4</sub> (0.82 mg, 0.21 mmol) in 10 ml of water. The resulting precipitate was obtained, collected by filtration and dried. Single crystal of 1 was obtained by slow diffusion of in stoichiometric quantities of pyridine-4-boronic acid hydrochloride and [Pt(CN)<sub>4</sub>] salt reagent. Yield % 71. Elemental analysis (%). Found: C, 30.74; H, 2.58; N, 15.36. Calculated: C, 29.40; H, 2.64; N, 14.80.

### Hirshfeld Surface Analysis (HS)

Hirshfeld surface analysis was carried out to identify the intermolecular interactions within the structure. Input file for Hirshfeld surface analysis was generated on CrystalExplorer (Wolff et al., 2013) using the Crystallographic Information File (CIF) file. Intermolecular interactions in a crystal structure using 3D HS and 2D fingerprint plots was verified. HS defines a volume around a molecule like a van der Waals surface or an outer surface of the electron density (Spackman and Jayatilaka, 2009).

### Computational Procedure

Quantum mechanical calculations were performed on Gaussian09W (Frisch et al., 2009) package program using DFT with the B3LYP (Becke, 1993) hybrid functional. Since the studied molecules contain heavy atoms, different basis sets are used for Pt and others. While Lanl2DZ (Becke, 1988) basis set was used in all calculations for the Pt atom, for other atoms 6-31G\* (Hehre et al., 1972) basis set is used for geometry optimizations, and 6-311G(d,p) (Krishnan et al., 1980) is used for energy and Natural Bond Orbital (NBO) calculations (Glendening et al., 2003). Fragment and charge decomposition analysis also performed using the AOMix (Gorelsky et al., 2006) package which uses as the input of the NBO outputs from G09.

## RESULTS AND DISCUSSION

The structure of [HNC<sub>5</sub>H<sub>4</sub>B(OH)<sub>2-4</sub>][PtCN<sub>4</sub>] (1) compound contains the expected planar anions of [PtCN<sub>4</sub>] and 4-pyridine boronic acid cations. On the other hand, the hydrogen atoms of the boronic acids in 1 is syn-anti conformation as shown in Scheme 1, which is convenient for the formation of a pair of charge-assisted hydrogen bonds with the N-atoms of [PtCN<sub>4</sub>] anion.

Compound 1 crystallizes in the monoclinic P2<sub>1</sub>/c space group (Table 1). The asymmetric unit of 1 contains a protonated acridine cation and one half of a [Pt(CN)<sub>4</sub>]<sup>2-</sup> anion. The Pt<sup>II</sup> ion in the anion of 1 is four-coordinated by four CN bounds and located on an inversion centre (see Figure 1). The cis C-Pt-C bond angles are 88.80(15)° and 91.20(15)° for 1, which deviates from the ideal square geometry angle (90°). Therefore, the coordination of each Pt<sup>II</sup> ion is described as slightly distorted square planar geometry. The Pt-C bond lengths are nearly equivalent [1.981(4) Å and 1.999(3) Å for 1] (Table 2). The anions are almost linear displaying Pt-C-N average bond angles of 177.79° for 1.

The sums of the angles around the boron (B1) atoms located on the pyridine ring are  $360^\circ$  (Table 2). On the other hand, the average B–C and B–O bond length of **1** is 1.6035 (5) Å and 1.3515(5) Å which are comparable to those of the previously reported similar systems (Parry et al., 2002).

The  $[\text{Pt}(\text{CN})_4]^{2-}$  anion is connected to pyridinium boronic acid cations via four  $\text{B}(\text{OH})\cdots\text{NCPT}^-$  and two  $\text{N-H}\cdots\text{NCPT}^-$  hydrogen bond interactions in **1** (Figure 1b). The two  $\text{B}(\text{OH})\cdots\text{NCPT}^-$  hydrogen bonds ( $\text{H}\cdots\text{N}$ , 1.95 Å;  $\text{O}\cdots\text{N}$ , 2.77 Å, and 2.81 Å;  $153^\circ$  and  $170^\circ$ ) in **1** indicates relatively strong interactions (Table 3). Because these hydrogen bond lengths are much shorter than the sum of the standard van der Waals radii (Bondi, 1964). All of the remaining hydrogen bond interaction geometries are within predetermined limits (Bondi, 1964). The primary hydrogen bonding motifs of **1** (Figure 2a) are ribbons with the parallel orientation of the pyridinium boronic acid cations that are linked by  $[\text{Pt}(\text{CN})_4]^{2-}$  anions having an approximate parallel orientation to the mean planes of the pyridine rings. These hydrogen-bonded ribbons form a 1-D supramolecular chain that runs parallel to along the b axis for **1**. Pt $\cdots$ Pt separations within hydrogen-bonded ribbon are 14.650 Å for **1**. The coordinating functions of the pyridinium boronic acid molecules are directed alternately above and below the corresponding glide plane (Campos-Gaxiola et al., 2010). Therefore, the 1-D networks of **1** are arranged as double ribbons in a parallel fashion in the bc plane and forming 2D networks (Figure 2c). Additionally, double ribbons motifs with  $\text{O-H}\cdots\text{N}$ ,  $\text{C-H}\cdots\text{O}$ ,  $\text{C-H}\cdots\text{N}$ , and  $\text{N-H}\cdots\text{N}$  hydrogen bond interactions generate 3-D hydrogen-bonded networks (Figure 2d).

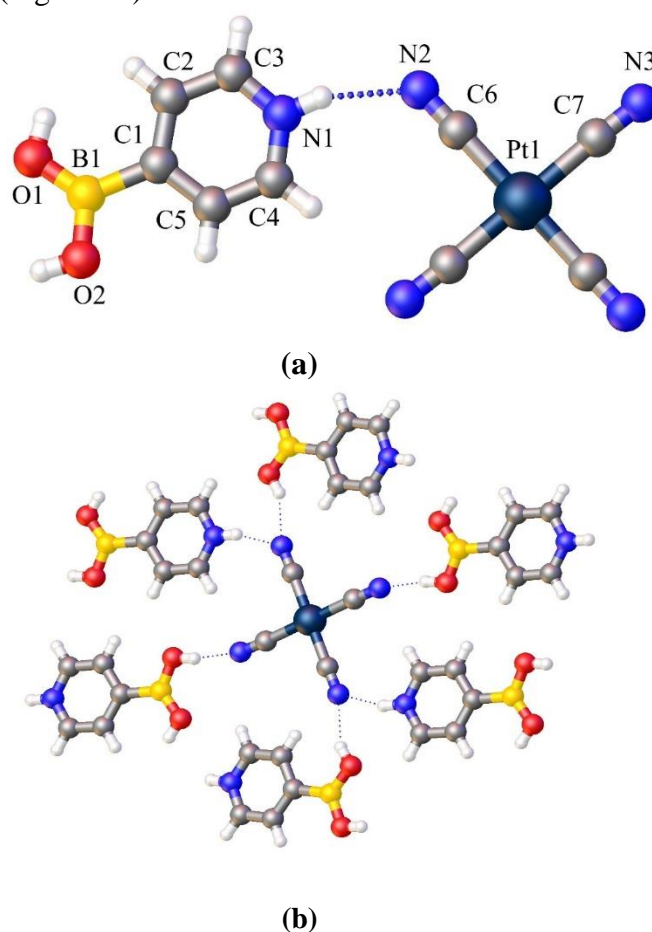


**Figure 1.** (a) View of the structure of **1** (b) The arrangement of hydrogen-bonded cations around the  $[\text{PtCN}_4]^{2-}$  anion in **1**.

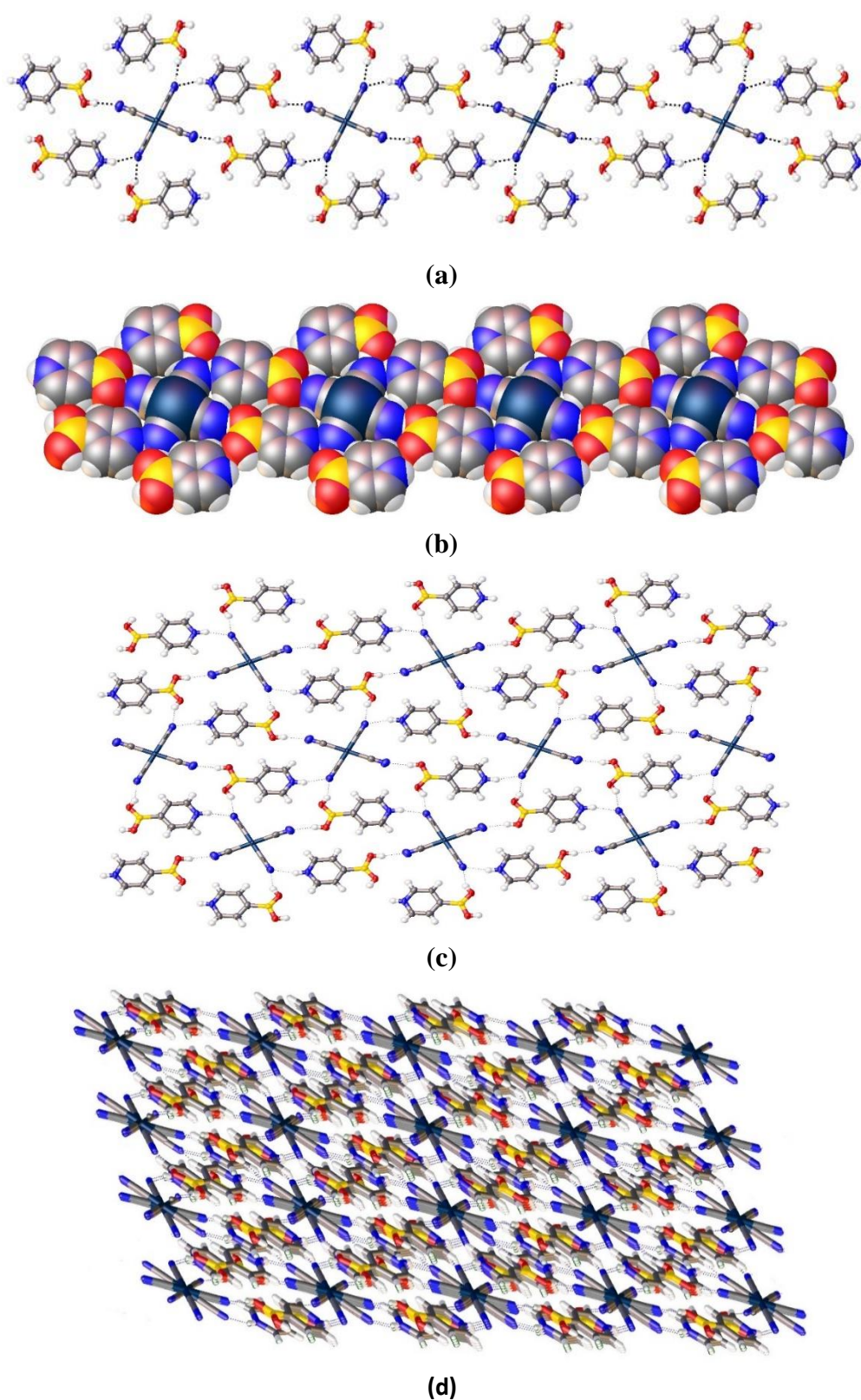


**Figure 2.** (a) 1-D chain view with  $\text{B}(\text{OH}) \cdots \text{NCpt}^-$  and  $\text{N}-\text{H} \cdots \text{NCpt}^-$  hydrogen-bonded of **1** (b) Space-filling representation of **1** (c) 2D network of **1** in the  $bc$  plane (d) 3D packing of the hydrogen-bonded network of **1**.

**Table 1.** Crystallographic information for **1**

	<b>1</b>
CCDC	2054948
Chemical Formula	C <sub>4</sub> N <sub>4</sub> Pt, 2(C <sub>5</sub> H <sub>7</sub> BNO <sub>2</sub> )
Crystal System	Monoclinic
Space Group	P2 <sub>1</sub> /c
Molecular Weight (gmol <sup>-1</sup> )	547.02
Unit cell parameter	<i>a</i> = 5.616(11) Å
	<i>b</i> = 14.656(3) Å
	<i>c</i> = 11.619(2) Å
	$\alpha = \gamma = 90^\circ$ $\beta = 110.35(3)^\circ$
V (Å <sup>3</sup> )	896.6(3)
T (K)	173(2)
Z	2
<i>d</i> (g/cm <sup>-3</sup> )	2.026
$\mu$ (mm <sup>-1</sup> )	7.859
Reflections collected	6 172
Independent reflections (R <sub>int</sub> )	2 050 [R <sub>int</sub> = 0.086]
Final R <sub>1</sub> [I > 2σ(I)], wR <sub>2</sub>	0.0306, 0.0701

**Table 2.** Selected geometric parameters of **1**. Given values are compared to X-ray crystallographic and computational results.

Bond Distances	Bond Angles				
	X-ray	Optimized	X-ray	Optimized	
Pt1-C6	1.981(4)	1.997	C6-Pt1-C7a	88.80(15)	85.93
Pt1-C7	1.999(3)	2.017	C6-Pt1-C7	91.20(15)	93.80
N1-C4	1.341(6)	1.346	C6-Pt1-C6a	180.00	179.7
N1-C3	1.333(5)	1.343	O1-B1-O2	120.8(4)	119.1
N2-C6	1.149(5)	1.169			
O1-B1	1.346(5)	1.366			
O2-B1	1.358(6)	1.364			
C1-B1	1.607(6)	1.580			

**Table 3.** Hydrogen-bond parameters of **1**

D-H...A*	D-H	H...A	D...A	D-H...A	Symmetry
N1-H1...N2	0.87	2.02	2.85	161	
O1-H1A...N2	0.84	2.03	2.81	153	-x,1/2+y,3/2-z
O2-H2A...N3	0.84	1.95	2.77	170	x,1+y,z
C2-H2...N2	0.95	2.48	3.39	163	-x,1/2+y,3/2-z
C3-H3...O1	0.95	2.52	3.17	126	-x,-1/2+y,3/2-z
C5-H5...O2	0.95	2.57	2.90	101	
C5-H5...O2	0.95	2.59	3.33	136	1-x,2-y,1-z

### Hirshfeld Surface Analysis of **1**

Hirshfeld surfaces (HS) of **1** with mapped  $d_{\text{norm}}$  is illustrated in Figure 3. Over the Hirshfeld surfaces, the inter-contacts included in hydrogen bonds are represented by red spots. The surfaces of 3D  $d_{\text{norm}}$  are plotted over a fixed colour scale of  $-0.6409 \text{ \AA}$  (red) to  $1.0748 \text{ \AA}$  (blue) with a standard (high) surface resolution for **1**. The surfaces are shown as transparent to allow visualization of the molecules. The vivid red spots are due to dominant  $\text{N}\cdots\text{H}$  distances corresponding to  $\text{N}-\text{H}\cdots\text{N}$  and  $\text{O}-\text{H}\cdots\text{N}$  interactions. The characteristics of the surfaces verify the dominant role of the hydrogen bonds in the solid-state packing. The 2D fingerprint plots for **1** are depicted in Figure 4. For **1**, the interactions in between the  $\text{N}\cdots\text{H}$  are featured by the spikes in the donor and acceptor sites of the fingerprint graph with  $d_e + d_i \approx 1.8 \text{ \AA}$  (32.2%). The contributions to the HS due to  $\text{H}\cdots\text{H}$  contacts are 14.8% in **1**.

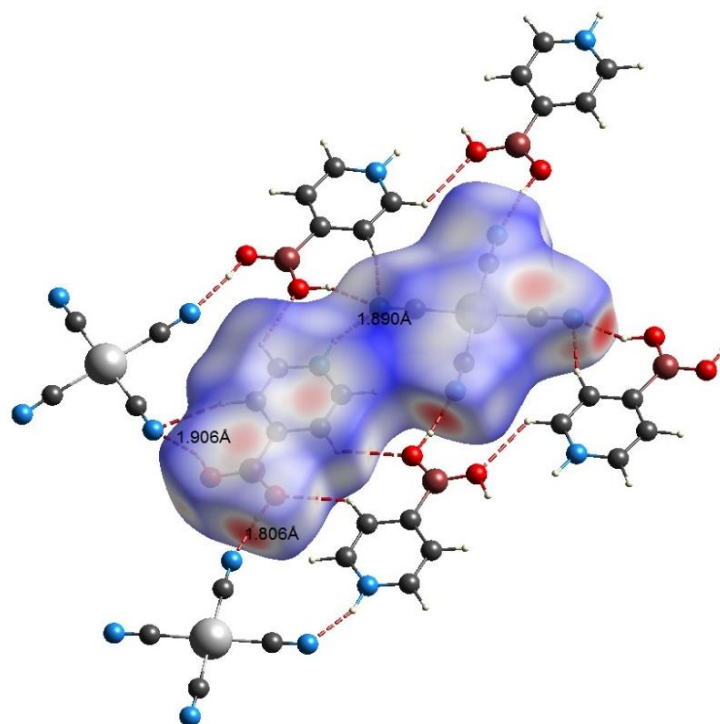


**Figure 3.** The red circular collapsing on the  $d_{\text{norm}}$  surface for visualizing the intermolecular contacts of **1**.

### Computational Results

Due to the symmetry, the asymmetric unit consists of half of the studied structure, but the whole structure was considered in the calculation. All geometric parameters are in good agreement with crystallographic and computational results as shown in Table 2.

Since low dependency on the basis sets, NBO charges are calculated. Although the formal charge of Pt moiety is  $-2e$ , the calculated charge is  $-1.70e$ . In **1**; Pt moiety donates  $-0.15e$  to each pyridinium boronic cations.

To examine the charge decomposition analysis in detail, the studied compound was considered in 3 fragments. 1<sup>st</sup> fragment is  $\text{C}_4\text{N}_4\text{Pt}$  part, 2<sup>nd</sup> and 3<sup>rd</sup> fragments are pyridinium boronic cations as shown in Figure 5. In **1**; Pt moiety donates  $0.397e$  and  $0.412e$  to neighbor fragments. There is an unremarkable back-donation to Pt moiety from other fragments in **1**. Due to the charge transfer on the whole compound is only from Pt moiety to pyridinium boronic cations, we can conclude the interaction between fragments is charge assisted.

Contributions of fragments molecular orbitals (HOFO-LUFO) to frontier molecular orbitals (HOMO-LUMO) of **1** are as follows (shown in Figure 5): Compound **1**: HOMO: 99.7% HOFO of Fragment 1. LUMO: 97.6% LUFO of Fragment 2, LUMO+1: 97.6% of Fragment 3. Considering the HOMO and LUMO of **1**, during the excitation of the compound, the charge is transferred from Pt moiety to other fragments.

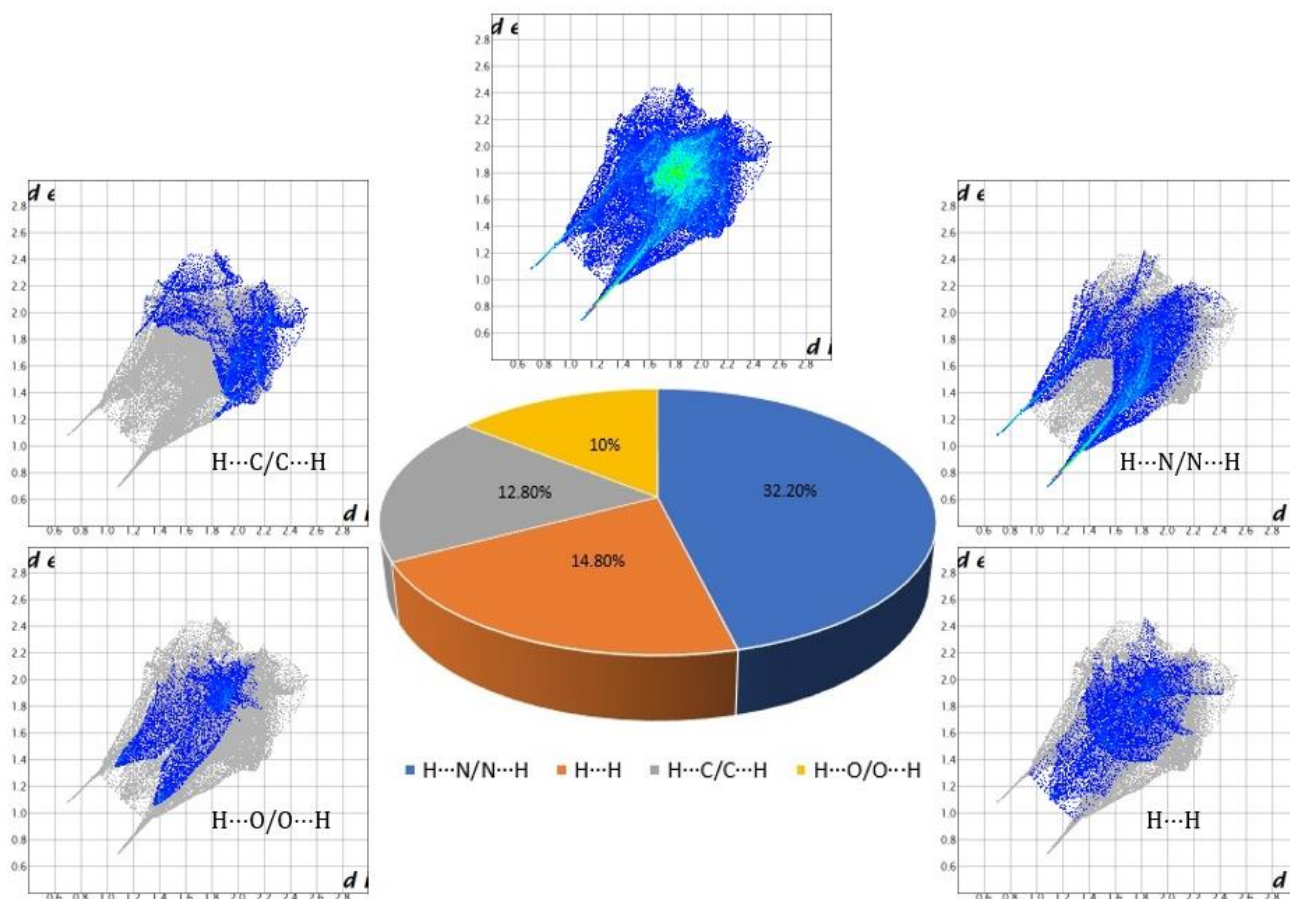


**Figure 4.** The contribution rates and 2D fingerprint plots of **1**.

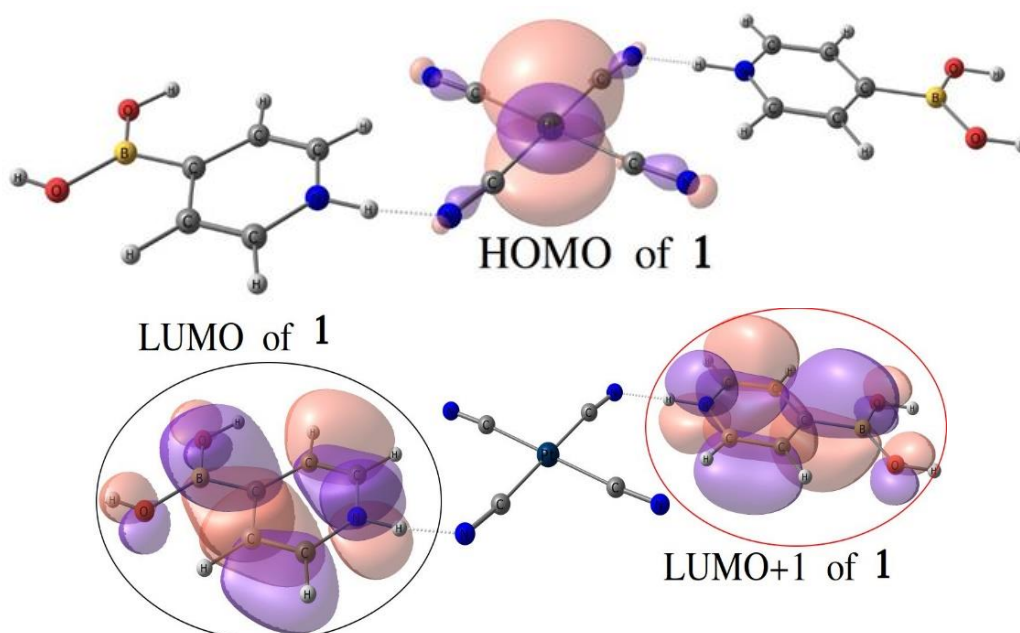


**Figure 5.** Frontier molecular orbitals of **1**. LUMO-HOMO energy gaps are 3.05 eV for **1**.

## CONCLUSION

In this study, a new compound [HNC<sub>5</sub>H<sub>4</sub>B(OH)<sub>2-4</sub>][Pt(CN)<sub>4</sub>] (**1**) has been investigated synthesis, crystal structure, geometry optimizations, and HOMO and LUMO molecular orbitals by the use of quantum chemical calculations. In the crystal structure of **1** found formation charge-assisted -B(OH)···NCp<sup>+</sup> and N-H···NCp<sup>+</sup> hydrogen-bonded containing pyridinium boronic acid. The O-H···N, C-H···O, C-H···N, and N-H···N hydrogen bond interactions also play a significant role in stabilizing the resulting 2D and 3D supramolecular networks. Also, analyses of intermolecular interactions in the crystal structure of **1** have been performed by visualizing Hirshfeld surface and 2D fingerprint plots.

## ACKNOWLEDGEMENTS

The authors thank to Professor Guy Orpen (School of Chemistry, Bristol University, England) for the use of the X-ray diffractometer.

## Conflict of Interest

The authors declare that they have contributed equally to the article.

## Author's Contributions

The article authors declare that there is no conflict of interest between them.

## REFERENCES

- Becke AD, 1988. Density-functional Exchange-Energy Approximation with Correct Asymptotic Behavior. *Physical Review A*, 38: 3098–3100.
- Becke AD, 1993. Density-Functional Thermochemistry. III. The Role of Exact Exchange. *The Journal of Physical Chemistry* 98: 5648–5652.
- Bondi A, 1964. Van der Waals Volumes and Radii. *The Journal of Physical Chemistry*, 68: 441–451.
- Campos-Gaxiola JJ, Vega-Paz A, Román-Bravo P, Höpfl H, Sánchez-Vázquez M, 2010. Pyridineboronic Acids as Useful Building Blocks in Combination with Perchloroplatinate(II) and -(IV) Salts: 1D, 2D, and 3D Hydrogen-Bonded Networks Containing X-H···Cl<sub>2</sub>Pt<sup>-</sup> (X=C,N<sup>+</sup>), B(OH)<sub>2</sub>···Cl<sub>2</sub>Pt<sup>-</sup>, and B(OH)<sub>2</sub>···(HO)<sub>2</sub>B Synthons. *Crystal Growth and Design*, 10: 3182–3190.
- Carvajal N, Uribe E, Sepu'lveda M, Mendoza C, Fuentealba B, Salas M, 1996. Chemical Modification of Semele Solida Arginase by Diethyl Pyrocarbonate: Evidence for A Critical Histidine Residue. *Comparative Biochemistry Physiology Part B: Biochemistry and Molecular Biology*, 114: 367–370.
- Coban MB, Erkarlan U, Oylumluoglu G, Aygun M and Kara H, 2016. Hydrothermal synthesis, crystal structure and Photoluminescent properties; 3D Holmium(III) coordination polymer. *Inorganica Chimica Acta*, 447: 87–91.
- Crystal Explorer 3.0, Wolff SK, Grimwood DJ, McKinnon JJ, Turner MJ, Jayatilaka D, Spackman MA, 2013.
- Deagostino A, Protti N, Alberti D, Boggio P, Bortolussi S, Altieri S, Crich SG, 2016. Insights Into The Use of Gadolinium and Gadolinium/Boron-Based Agents in Imaging-Guided Neutron Capture Therapy Applications. *Future Medicinal Chemistry*, 8: 899–917.
- Deng Q, Zheng Q, Zuo B, Tu T, 2020. Robust NHC-Palladacycles-Catalyzed Suzuki–Miyaura Cross-Coupling of Amides Via C-N Activation. *Green Synthesis and Catalysis*, 1: 75–78.
- Diccianni JB, Diao T, 2019. Mechanisms of Nickel-Catalyzed Cross-Coupling Reactions. *Trends in Chemistry*, 1: 830–844.

- Dolomanov OV, Bourhis LJ, Gildea RJ, Howard JAK, Puschmann H, 2009. OLEX2 : A Complete Structure Solution, Refinement and Analysis Program. *Journal of Applied Crystallography*, 42: 339–341.
- Ejsmont K, Zaleski J, Sporyński A, Lewandowski M, 2003. 5-Formyl-2-Furanboronic Acid at 100 K. *Acta Crystallographica Section E: Structure Reports Online*, 59: o1324–o1326.
- Erkarslan U, Oylumluoglu G, Coban MB, Ozturk E and Kara H, 2016. Cyanide-bridged trinuclear MnIII–FeIII assembly: Crystal structure, magnetic and photoluminescence behavior. *Inorganica Chimica Acta*, 445: 57–61.
- Erkarslan U, Donmez A, Kara H, Aygun M and Coban MB, 2018. Synthesis, Structure and Photoluminescence Performance of a New Er<sup>3+</sup> Cluster-Based 2D Coordination Polymer. *Journal of Cluster Science*, 29: 1177–1183.
- Gaussian 09w, Frisch MJ, Trucks GW, Schlegel HB, Scuseria GE, Robb MA, Cheeseman JR, Scalmani G, Barone V, Petersson GA, Nakatsuji H, Li X, Caricato M, Marenich AV, Bloino J, Janesko BG, Gomperts R, Mennucci B, Hratchian HP, Ortiz JV, Izmaylov AF, Sonnenberg JL, Willia FD, 2009.
- Glendening ED, Reed AE, Carpenter, JE, Weinhold F, 2003. NBO Version 3.1. Gaussian Inc., Pittsburgh.
- Gorelsky SI, Ghosh S, Solomon EI, 2006. Mechanism of N<sub>2</sub>O Reduction by the  $\mu_4$ -S Tetranuclear CuZ Cluster of Nitrous Oxide Reductase. *Journal of the American Chemical Society*, 128: 278–290.
- Hall DG, 2011. Boronic Acids: Preparation and Applications in Organic Synthesis, Medicine and Materials, (Volume 1 and 2).
- Hehre WJ, Ditchfield R, Pople JA, 1972. Self-Consistent Molecular Orbital Methods. XII. Further Extensions of Gaussian-Type Basis Sets for Use in Molecular Orbital Studies of Organic Molecules. *Journal of Chemical Physics*, 56: 2257–2261.
- Kara H, Adams CJ, Orpen, AG, Podesta TJ, 2006. Pyridinium Boronic Acid Salts in Crystal Synthesis. *New Journal of Chemistry*, 30: 1461–1469.
- Khangulov SV, Pessiki, PJ, Barynin VV, Ash DE, Dismukes GC, 1995. Determination of the Metal Ion Separation and Energies of the Three Lowest Electronic States of Dimanganese(II,II) Complexes and Enzymes: Catalase and Liver Arginase. *Biochemistry*, 34: 2015–2025.
- Kocak C, Oylumluoglu G, Donmez A, Coban MB, Erkarslan U, Aygun M and Kara H, 2017. Crystal structure and photoluminescence properties of a new monomeric copper (II) complex: bis (3-[(3-hydroxypropyl) imino] methyl)-4-nitrophenolato- $\kappa^3$ O,N,O') copper (II). *Acta Crystallographica Section C: Structural Chemistry*, 73: 414–419.
- Krishnan R, Binkley JS, Seeger R, Pople JA, 1980. Self-Consistent Molecular Orbital Methods. XX. A Basis Set for Correlated Wave Functions. *Journal of Chemical Physics*, 72: 650–654.
- Kumar M, Jha A, Dr M, Mishra B, 2020. Targeted Drug Nanocrystals for Pulmonary Delivery: A Potential Strategy for Lung Cancer Therapy. *Expert Opinion on Drug Delivery*, 1–14.
- Li B, Li T, Aliyu MA, Li ZH, Tang W, 2019. Enantioselective Palladium-Catalyzed Cross-Coupling of  $\alpha$ -Bromo Carboxamides and Aryl Boronic Acids. *Angewandte Chemie*, 201905174.
- Miyaura N, Suzuki A, 1995. Palladium-Catalyzed Cross-Coupling Reactions of Organoboron Compounds. *Chemical Reviews*, 95: 2457–2483.
- Mohammadi M, Ghorbani-Choghamarani A, 2020. l-Methionine–Pd Complex Supported on Hercynite As A Highly Efficient and Reusable Nanocatalyst for C–C Cross-Coupling Reactions. *New Journal of Chemistry*, 44: 2919–2929.

- Parry PR, Wang C, Batsanov AS, Bryce MR, Tarbit B, 2002. Functionalized Pyridylboronic Acids and Their Suzuki Cross-Coupling Reactions to Yield Novel Heteroarylpyridines. *Journal of Organic Chemistry*, 67: 7541–7543.
- Roughley SD, Jordan AM, 2011. The Medicinal Chemist's Toolbox: An Analysis of Reactions Used in the Pursuit of Drug Candidates. *Journal of Medicinal Chemistry*, 54: 3451–3479.
- SeethaLekshmi N, Pedireddi VR, 2007. Solid-State Structures of 4-Carboxyphenylboronic Acid and Its Hydrates. *Crystal Growth and Design*, 7: 944–949.
- Sheldrick GM, 2008. A Short History of SHELX. *Acta Crystallographica*, A64: 112–122.
- Spackman MA, Jayatilaka D, 2009. Hirshfeld Surface Analysis. *CrystEngComm*, 11: 19–32.
- Suzuki A, Diederich F, Stang PJ, 1998. *Metal-catalyzed Cross-coupling Reactions* Wiley-VCH, Weinheim, Germany, Chapter 2.
- Torborg C, Beller M, 2009. Recent Applications of Palladium-Catalyzed Coupling Reactions in the Pharmaceutical, Agrochemical and Fine Chemical Industries. *Advanced Synthesis Catalysis*, 351: 3027–3043.
- SAINT V7.60A, Bruker-AXS 2008. Inc. Madison, Wisconsin, USA.
- Varughese S, Sinha, SB, Desiraju GR, 2011. Phenylboronic Acids in Crystal Engineering: Utility of The Energetically Unfavorable Syn,Syn-Conformation in Co-Crystal Design. *Science China Chemistry*, 54: 1909–1919.
- Yahsi Y, Gungor E, Kara H, 2015. Chlorometallate-Pyridinium Boronic Acid Salts for Crystal Engineering: Synthesis of One-, Two- and Three-Dimensional Hydrogen Bond Networks. *Crystal Growth and Design*, 15: 2652–2660.
- Yang W, Gao X, Springsteen G, Wang B, 2002. Catechol Pendant Polystyrene for Solid-Phase Synthesis. *Tetrahedron Letter*, 43: 6339–6342.
- Yang W, Gao X, Wang B, 2003. Boronic Acid Compounds as Potential Pharmaceutical Agents. *Medical Research Reviews*, 23: 346–368.
- Zhu Q, Saeed M, Song R, Sun T, Jiang C, Yu H, 2020. Dynamic Covalent Chemistry-Regulated Stimuli-Activatable Drug Delivery Systems for Improved Cancer Therapy. *Chinese Chemical Letter*, 31: 1051–1059.